

Evolution of platinum anticancer

agents: Research into platinum-based anticancer compounds has led to the development of a myriad of drugs, with only a small handful gaining approval. This review highlights the current techniques for improving these approved drugs to retain or improve efficacy whilst reducing toxic side effects. We focus on cancer-specific targeting, drug delivery and the prodrug approach.



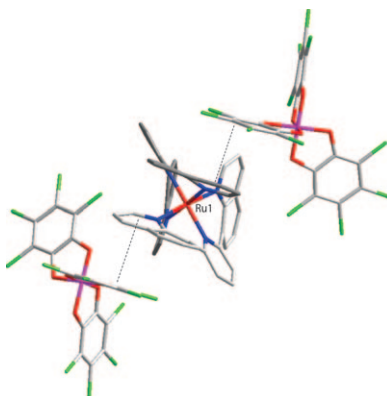
Drug Delivery

B. W. Harper, A. M. Krause-Heuer, M. P. Grant, M. Manohar, K. B. Garbutcheon-Singh, J. R. Aldrich-Wright 7064–7077*

Advances in Platinum Chemotherapeutics

COMMUNICATIONS

Resolving the problem! The conformationally chiral bistridentate $[\text{Ru}(\text{dqp})_2]^{2+}$ complex ($\text{dqp} = 2,6\text{-di}(\text{quinolin-8-yl})\text{pyridine}$) was resolved by selective precipitation using $[\Delta\text{-TRISPHAT}]^-$ (tris(tetrachlorocatecholate)phosphate) as the chiral auxiliary. The X-ray crystal structure of one diastereomer has been solved (see picture). No evidence for racemization was observed either at elevated temperature or with visible light.



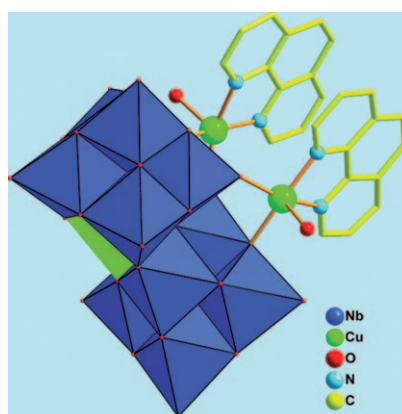
Chirality

S. Sharma, F. Lombeck, L. Eriksson, O. Johansson 7078–7081*

Resolution of Conformationally Chiral $mer\text{-}[\text{Ru}(\text{dqp})_2]^{2+}$ and Crystallographic Analysis of $[\delta,\delta\text{-Ru}(\text{dqp})_2][\Delta\text{-TRISPHAT}]_2$ ($\text{dqp} = 2,6\text{-Di}(\text{quinolin-8-yl})\text{pyridine}$; TRISPHAT = Tris(tetrachlorocatecholate)phosphate)



Keep it in the family: Two novel copper–undecaniobates $[\{\text{Cu}(\text{H}_2\text{O})\text{L}\}_2\{\text{CuNb}_{11}\text{O}_{35}\text{H}_4\}]^{5-}$ ($\text{L} = 1,10\text{-phenanthroline}$ or $2,2'\text{-bipyridine}$, an example is shown here) have been successfully synthesized by the diffusion strategy and, as far as we know, represent the first examples of copper–undecaniobates in the polyoxoniobate family.



Polyoxometalates

J.-Y. Niu, G. Chen, J.-W. Zhao, P.-T. Ma, S.-Z. Li, J.-P. Wang, M.-X. Li, Y. Bai, B.-S. Ji . . . 7082–7086*

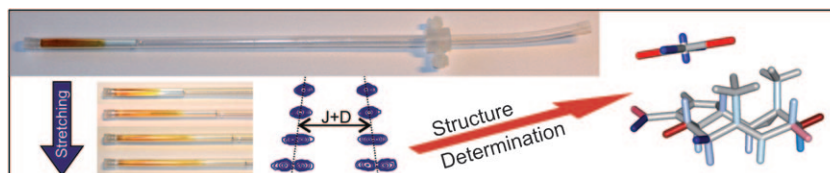
Two Novel Copper–Undecaniobates Decorated by Copper–Organic Cations $[\{\text{Cu}(\text{H}_2\text{O})\text{L}\}_2\{\text{CuNb}_{11}\text{O}_{35}\text{H}_4\}]^{5-}$ ($\text{L} = 1,10\text{-phenanthroline}$, $2,2'\text{-bipyridine}$) Consisting of Plenary and Monolacunary Lindqvist-Type Isopolyniobate Fragments



NMR Spectroscopy

G. Kummerlöwe, E. F. McCord,
S. F. Cheatham, S. Niss, R. W. Schnell,
B. Luy* 7087–7089

Tunable Alignment for All Polymer Gel/Solvent Combinations for the Measurement of Anisotropic NMR Parameters



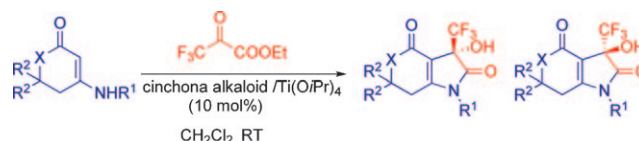
A **stretching apparatus** (see figure) with arbitrary scalability of alignment strength is introduced for the measurement of anisotropic NMR parameters, which works for practically all polymer gel/solvent combinations. Its use is

demonstrated in applications involving the steady incrementation of residual dipolar couplings, the distinction of enantiomers, and the conformational analysis of organic compounds.

Asymmetric Synthesis

S. Ogawa, N. Iida, E. Tokunaga,
M. Shiro, N. Shibata* 7090–7095

Cinchona Alkaloid/Ti^{IV}-Catalyzed Enantioselective Enamine–Trifluoropyruvate Condensation–Cyclization Reaction and Its Application to Drug-like Heterocycles



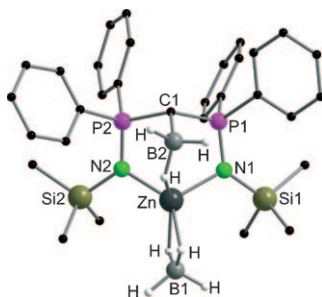
Drug design: A cinchona alkaloid/Ti^{IV}-catalyzed enantioselective tandem enamine–trifluoropyruvate condensation–cyclization reaction provides a robust method for the construction of small heterocyclic molecules with a

quaternary trifluoromethylated carbon center (see scheme). The series of products are attractive templates and were readily converted to drug-like trifluoromethylated heterocycles by conventional methods.

BH₃ Coordination

S. Marks, R. Köppe, T. K. Panda,
P. W. Roesky* 7096–7100

Unprecedented Zinc–Borane Complexes

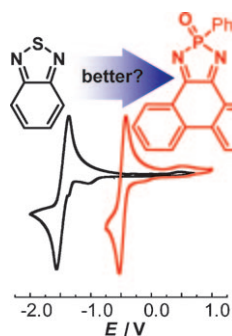


A **borane–borohydride** and a borane–methyl zinc complex were synthesized by different synthetic pathways. In both compounds the borane molecule is κ^1 -coordinated to the zinc atom (see figure).

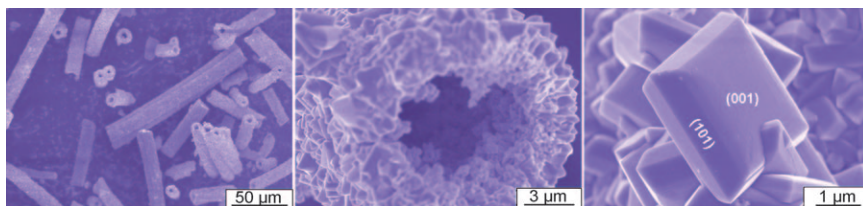
Phosphorus Heterocycles

T. Linder, T. C. Sutherland,*
T. Baumgartner* 7101–7105

Extended 2,5-Diazaphosphole Oxides: Promising Electron-Acceptor Building Blocks for π -Conjugated Organic Materials



BTD makeover—phosphorus edition: Replacing the sulfur atom in π -extended 2,1,3-benzo[*c*]thiadiazoles (BTD) by a phosphoryl group affords the materials with improved electron-acceptor properties. The significantly lower reduction potentials and competitive electron-transfer rates make the new diazaphosphole oxides excellent candidates for application in π -conjugated organic materials (see figure).



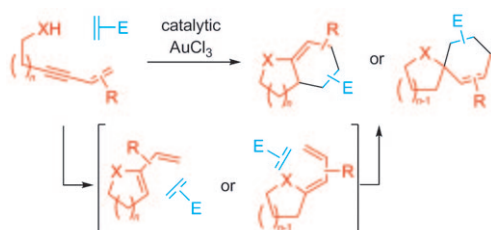
Amazing anatase: Anatase TiO₂ tubular structures made up of microcrystallites with a high percentage of {001} facets were synthesized by a simple one-step hydrothermal process with ZrO₂ fibers as a template (see

graphic). The morphologies, structures and growth procedures were systematically investigated, and a plausible mechanism for the formation of these structures was proposed.

Hydrothermal Synthesis

X. Wang, B. Huang, Z. Wang, X. Qin, X. Zhang, Y. Dai, M.-H. Whangbo* 7106–7109

Synthesis of Anatase TiO₂ Tubular Structures Microcrystallites with a High Percentage of {001} Facets by a Simple One-Step Hydrothermal Template Process



Running rings around gold: A new cascade reaction catalysed by AuCl₃ that is based upon an initial cycloisomerisation reaction of enynol or enynamine derivatives, which form 1,3-butadiene derivatives, followed by a Diels–Alder cycloaddition reaction to give fused or spirocyclic compounds is reported (see scheme).

diene derivatives, followed by a Diels–Alder cycloaddition reaction to give fused or spirocyclic compounds is reported (see scheme).

Homogeneous Catalysis

J. Barluenga, J. Calleja, A. Mendoza, F. Rodríguez, F. J. Fañanás* 7110–7112

Synthesis of Polycyclic Compounds by a Cascade Cycloisomerisation/Diels–Alder Reaction

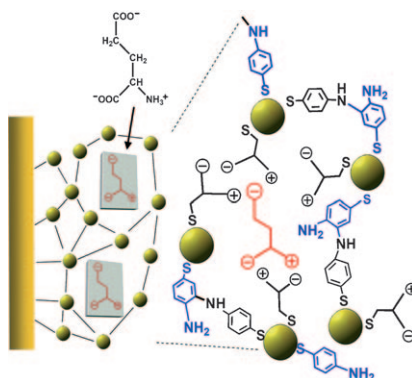
FULL PAPERS

Molecular Imprinting

*M. Riskin, R. Tel-Vered, M. Frasconi, N. Yavo, I. Willner** 7114–7120

Stereoselective and Chiroselective Surface Plasmon Resonance (SPR) Analysis of Amino Acids by Molecularly Imprinted Au-Nanoparticle Composites

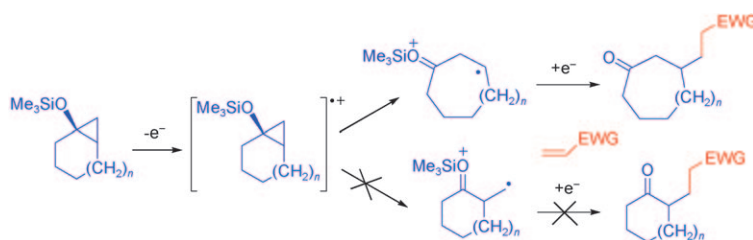
Au-nanoparticle composites detect amino acids: Selective and chiroselective surface plasmon resonance (SPR) analysis of amino acids is accomplished with molecularly imprinted bis-aniline-crosslinked Au-nanoparticle composites electropolymerized on Au surfaces (see graphic).



Radicals

H. Rinderhagen, J. Mattay,*
R. Nussbaum, T. Bally* . . . 7121–7124

**Regioselective Oxidative Ring
Opening of Cyclopropyl Silyl Ethers:
A Quantum Chemical Study**



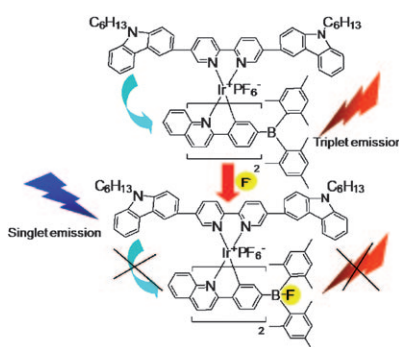
Spontaneous fragmentation is observed for cyclopropyl silyl ethers (see scheme), sometimes followed by re-cyclisation to form new products, in the absence of nucleophiles, that is, under conditions where alkyl- or aryl-

substituted cyclopropanes do not even epimerize. In cyclic systems intermolecular addition reactions lead predominantly to the *endo*-addition products, which is caused by the selectivity of the initial fragmentation.

Sensors

W.-J. Xu, S.-J. Liu, X.-Y. Zhao, S. Sun,
S. Cheng, T.-C. Ma, H.-B. Sun,
Q. Zhao,* W. Huang* 7125–7133

**Cationic Iridium(III) Complex
Containing both Triarylboron and
Carbazole Moieties as a Ratiometric
Fluoride Probe That Utilizes a Switchable
Triplet–Singlet Emission**

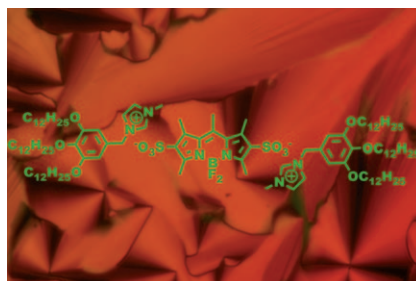


Probing for information: A fluoride probe based on a cationic Ir^{III} complex contains both triarylboron and carbazole moieties. Binding of F⁻ ions to the complex can quench the phosphorescent emission from the Ir^{III} complex and enhance the fluorescent emission from the N^N ligand, which corresponds to a visual change in the emission from orange/red to blue (see scheme). Thus, colorimetric and ratiometric fluoride sensing can be realized.

Ionic Liquid Crystals

J.-H. Olivier, F. Camerel, G. Ulrich,
J. Barberá,* R. Ziessel* 7134–7142

**Luminescent Ionic Liquid Crystals
from Self-Assembled BODIPY Disul-
fonate and Imidazolium Frameworks**

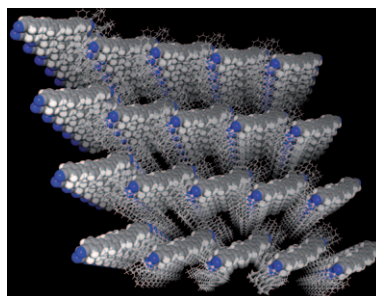


Glow in the dark! Ionic self-assembly involving functionalized imidazolium cations and 4,4-difluoro-4-bora-3a,4a-diaza-*s*-indacene-2,6-disulfonates produces columnar luminescent ionic liquid crystals (ILCs; see figure) over a wide temperature range and luminescent patterned films when acrylates replace some of the terminal methyl groups.

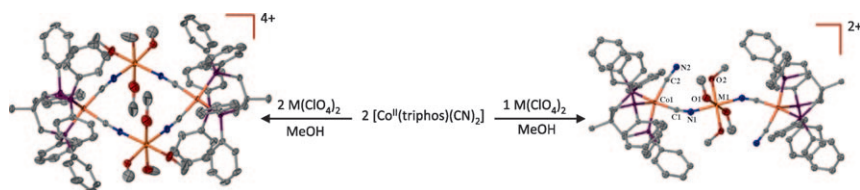
Supramolecular Chemistry

Y. Yao, W. Shen, B. Nohra, C. Lescop,*
R. Réau* 7143–7163

**Coordination-Driven Hierarchical
Organization of π -Conjugated
Systems: From Molecular to Supra-
molecular π -Stacked Assemblies**



Big is beautiful! A general approach to π -stacked supramolecular rectangles is described. The reaction of U-shaped, bimetallic, Cu^I complexes, assembled from a heteroditopic pincer, with cyano-capped π -conjugated linkers gives straightforward access to π -stacked metalocyclophanes in good yields. Rectangles based upon long π systems stack in the solid state along infinite columns of interacting π systems (see figure).



Subtle factors: Both trinuclear $[\text{Co}_2\text{M}]$ ($\text{M} = \text{Mn}, \text{Fe}, \text{Co}, \text{Ni}$) and tetranuclear $[\text{Co}_2\text{M}_2]$ ($\text{M} = \text{Mn}, \text{Ni}$) complexes were isolated from reactions of $[\text{Co}^{\text{II}}(\text{triphos})(\text{CN})_2]$ and $\text{M}(\text{ClO}_4)_2 \cdot 6\text{H}_2\text{O}$ in methanol (see scheme). The observa-

tion of antiferromagnetic or ferromagnetic coupling was rationalized by DFT calculations and found to derive from overlap patterns of the different magnetic orbitals as influenced by the angles of the cyanide bridges.

Cobalt Complexes

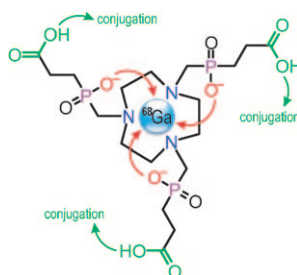
*F. Karadas, M. Shatruk, L. M. Perez, K. R. Dunbar** 7164–7173

Cyanide-Bridged $[\text{Co}^{\text{II}}_2\text{M}^{\text{II}}]$ and $[\text{Co}^{\text{II}}_2\text{M}^{\text{II}}_2]$ Complexes Based on the $[\text{Co}^{\text{II}}(\text{triphos})(\text{CN})_2]$ Building Block: Syntheses, Structures, Magnetic Properties, and Density Functional Theoretical Studies



Towards nuclear imaging tracers:

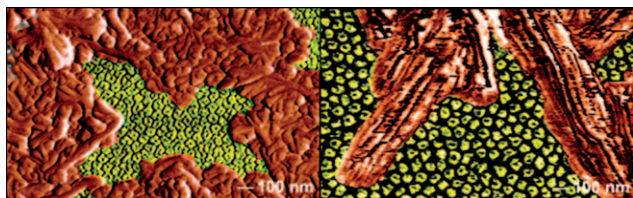
Rapid and selective formation of highly stable, kinetically inert Ga^{III} complexes over a wide pH range, together with the possibility to conjugate multiple biomolecules through amide bonds, render the ligand **PrP9** (see scheme) an ideal starting point for the synthesis of ^{68}Ga -based tracers for positron emission tomography (PET).



Radiopharmaceuticals

J. Notni, P. Hermann,* J. Havlíčková, J. Kotecký, V. Kubiček, J. Plutnar, N. Loktionova, P. J. Riss, F. Rösch, I. Lukeš* 7174–7185

A Triazacyclononane-Based Bifunctional Phosphinate Ligand for the Preparation of Multimeric ^{68}Ga Tracers for Positron Emission Tomography



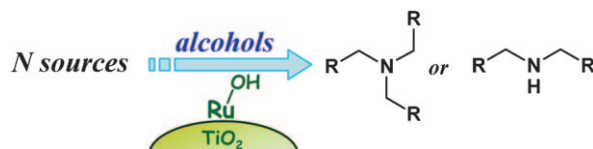
Under pressure: Films of self-assembled surface micelles of fluorocarbon/hydrocarbon diblocks can be compressed far beyond monolayer col-

lapse, which results in composite multi-layer or dendrite formation (see images). A regular monolayer of surface hemimicelles is preserved.

Film Compression

*C. de Gracia Lux, J.-L. Gallani, G. Waton, M. P. Krafft** 7186–7198

Compression of Self-Assembled Nano-Objects: 2D/3D Transitions in Films of (Perfluoroalkyl)Alkanes—Persistence of an Organized Array of Surface Micelles



Borrowing pays off in the end: The N-alkylation of ammonia (or its surrogates) and amines with alcohols to produce tertiary or secondary amines was efficiently promoted by the easily prepared and inexpensive supported

ruthenium hydroxide catalyst $\text{Ru}(\text{OH})_x/\text{TiO}_2$. This catalytic transformation proceeds through consecutive N-alkylation reactions, in which the alcohols act as alkylating reagents (see picture).

Heterogeneous Catalysis

*K. Yamaguchi, J. L. He, T. Oishi, N. Mizuno** 7199–7207

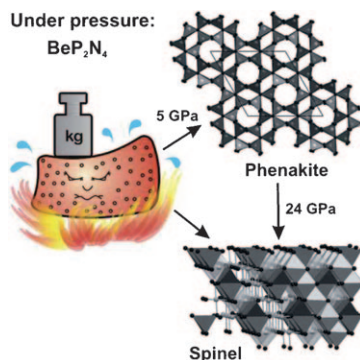
The “Borrowing Hydrogen Strategy” by Supported Ruthenium Hydroxide Catalysts: Synthetic Scope of Symmetrically and Unsymmetrically Substituted Amines



Hard Materials

F. J. Pucher, S. R. Römer, F. W. Karau, W. Schnick 7208–7214*

Phenakite-Type BeP_2N_4 —A Possible Precursor for a New Hard Spinel-Type Material

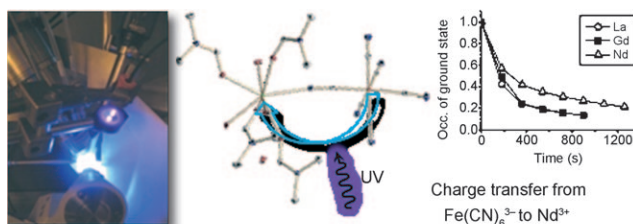


Hard as nails! BeP_2N_4 , a novel nitrido-phosphate crystallizing in the phenakite-type structure, was synthesized in a multi-anvil apparatus under high-pressure/high-temperature conditions (see picture). Remarkable structural and material properties are anticipated for spinel-type BeP_2N_4 .

Photocrystallography

H. Svendsen, J. Overgaard, M. A. Chevallier, E. Collet, Y.-S. Chen, F. Jensen, B. B. Iversen 7215–7223*

Photomagnetic Switching of Heterometallic Complexes $[\text{M}(\text{dmf})_4(\text{H}_2\text{O})_3(\mu\text{-CN})\text{Fe}(\text{CN})_5]\cdot\text{H}_2\text{O}$ ($\text{M} = \text{Nd, La, Gd, Y}$) Analyzed by Single-Crystal X-ray Diffraction and Ab Initio Theory



Making light of things: Single-crystal X-ray diffraction combined with UV illumination revealed the ground- and excited-state structures of photomagnetic heterobimetallic complexes $[\text{M}(\text{dmf})_4(\text{H}_2\text{O})_3(\mu\text{-CN})\text{Fe}(\text{CN})_5]\cdot\text{H}_2\text{O}$

($\text{M} = \text{Nd, La, Gd, Y}$). Theoretical analysis suggests that charge transfer from the cyano ligands to the lanthanide atoms explains the photomagnetic effect (see figure).

Structure Elucidation

D. Šišak, L. B. McCusker, A. Buckl, G. Wuitschik, Y.-L. Wu, W. B. Schweizer,* J. D. Dunitz* 7224–7230*

The Search for Tricyanomethane (Cyanoforn)

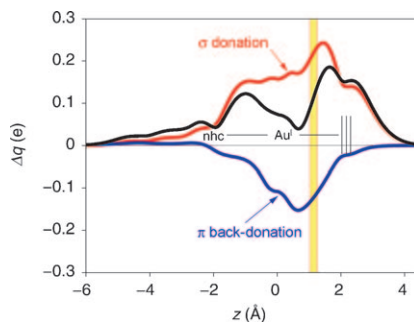


Surprise? In an attempt to prepare tricyanomethane, transfer of two molecules of water from concentrated sulfuric acid (!) to the dicyanoketenimine tautomer leads to the compound shown.

Coordination Modes

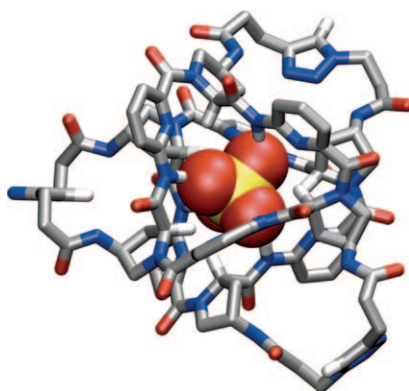
N. Salvi, L. Belpassi, F. Tarantelli 7231–7240*

On the Dewar–Chatt–Duncanson Model for Catalytic Gold(I) Complexes



Coordination bonds defined! A charge–displacement analysis reveals the full picture of σ donation and π back-donation in catalytic gold(I)–alkyne complexes (see figure; nhc = 2,3-dihydroimidazol-2-ylidene).

Encapsulated perfectly: A cage-type receptor that comprises two cyclopeptide subunits covalently linked through three linkers was assembled by using click chemistry (see picture). This receptor features a polar interior, because of a converging arrangement of the cyclopeptide NH groups, that enables tight binding to sulfate ions in an aqueous environment. Interestingly, complex stability is entirely due to the huge contribution of entropy to the complex formation.

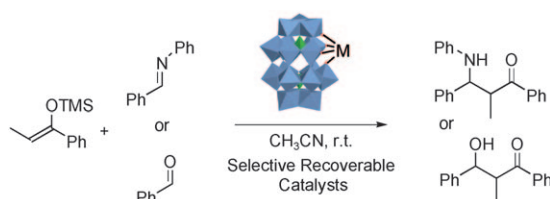


Host–Guest Systems

*T. Fiehn, R. Goddard, R. W. Seidel, S. Kubik** 7241–7255

A Cyclopeptide-Derived Molecular Cage for Sulfate Ions That Closes with a Click 


Forming bonds: It is proposed that organosoluble Lewis acidic polyoxo-metalates containing Zr, Sc, Y, Hf, or lanthanide atoms catalyze C–C bond-formation reactions, such as the Mannich and Mukaiyama-type reactions



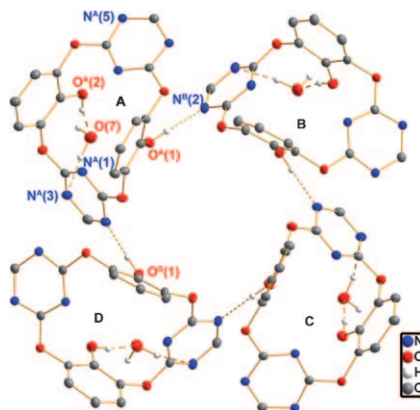
(see scheme; M = metal center). These air- and water-stable catalysts activate imines in a Lewis acidic way, whereas aldehydes are activated by indirect Brønsted catalysis.

C–C Coupling

N. Dupré, P. Rémy, K. Micoine, C. Boglio, S. Thorimbert, E. Lacôte,* B. Hasenknopf, M. Malacria* 7256–7264


Chemoselective Catalysis with Organosoluble Lewis Acidic Polyoxotungstates 

Heterocalixaromatics: Functionalised tetraoxacalix[2]arene[2]triazines have been synthesised efficiently by the fragment coupling approach under very mild conditions. A lower-rim dihydroxy-substituted tetraoxacalix[2]arene[2]triazine host molecule, which self-associates into a dimer in solution and a tetramer in the solid state (see figure), acts as a hydrogen-bond donor to form host–guest complexes with 2,2'-bipyridine, 4,4'-bipyridine and 1,10-phenanthroline both in solution and in the solid state.

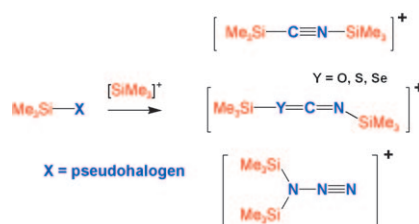


Host–Guest Systems

Q.-Q. Wang, D.-X. Wang, H.-B. Yang, Z.-T. Huang, M.-X. Wang** 7265–7275


Synthesis, Structure and Molecular Recognition of Functionalised Tetraoxacalix[2]arene[2]triazines 

Not only angels have halos: By utilizing a concept, which was first applied to halogens, to reaction mixtures such as $\text{Me}_3\text{Si-X}/[\text{Me}_3\text{Si-X-SiMe}_3]^+$ ($\text{X} = \text{CN}, \text{OCN}, \text{SCN}, \text{and NNN}$), it was possible to prepare the first bis-silylated pseudohalonium cations in high yields, thereby proving and extending the pseudohalogen concept.



Halogen Compounds

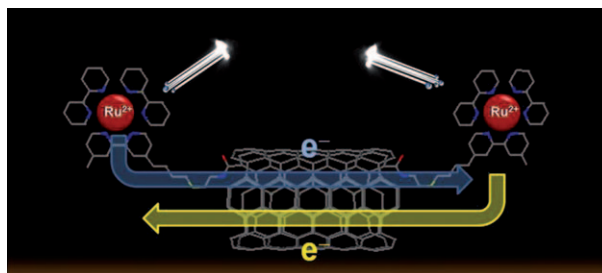
A. Schulz, A. Villinger** ... 7276–7281

Pseudohalonium Ions: $[\text{Me}_3\text{Si-X-SiMe}_3]^+$ ($\text{X} = \text{CN}, \text{OCN}, \text{SCN}, \text{and NNN}$) 

Photon Chemistry

R. Martín, L. Jiménez, M. Alvaro,
J. C. Scaiano, H. Garcia* ... 7282–7292

**Two-Photon Chemistry in Ruthenium
2,2'-Bipyridyl-Functionalized Single-
Wall Carbon Nanotubes**



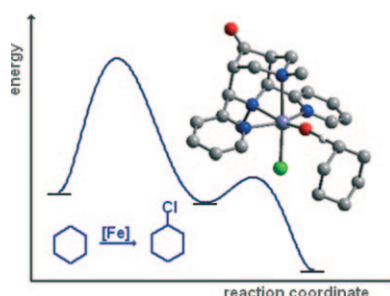
Ruthenium discotheque: A high-energy laser pulse combined with the long lifetime of $[\text{Ru}(\text{bpy})_3]^{2+}$ (bpy = 2,2'-bipyridyl) triplets and the low energy of the valence band in single-wall carbon nanotubes

(SWCNTs) leads to the formation of two distant triplet $[\text{Ru}(\text{bpy})_3]^{2+}$ excitons (see picture). A number of interesting photon-based mechanisms were revealed by using laser flash photolysis.

Enzyme Models

P. Comba,* S. Wunderlich . . 7293–7299

**Iron-Catalyzed Halogenation of
Alkanes: Modeling of Nonheme Halo-
genases by Experiment and DFT
Calculations**

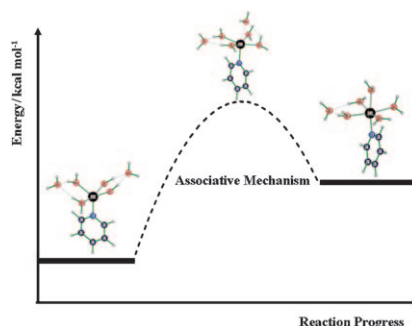


A range of routes: A highly active iron complex of tetradentate bispidine ligand L can selectively halogenate cyclohexane catalytically. Experimental and computational studies suggest different possible reaction pathways that strongly depend on the oxidant used for the reaction. The mechanism may involve Fe^{IV} and Fe^{V} oxo intermediates, for example, $[\text{Fe}^{\text{IV}}=\text{O}(\text{L})\text{Cl}]^+ \cdots \text{C}_6\text{H}_{12}$ (see picture; C gray, Cl green, Fe light blue, N dark blue, O red, H omitted except for $\text{FeO} \cdots \text{C}_6\text{H}_{12}$ interaction).

Reaction Mechanisms

B. M. Alzoubi, R. Puchta,*
R. van Eldik* 7300–7308

**Ligand-Exchange Processes on
Solvated Zinc Cations: Water
Exchange on $[\text{Zn}(\text{H}_2\text{O})_4(\text{L})]^{2+} \cdot 2\text{H}_2\text{O}$
(L = Heterocyclic Ligand)**

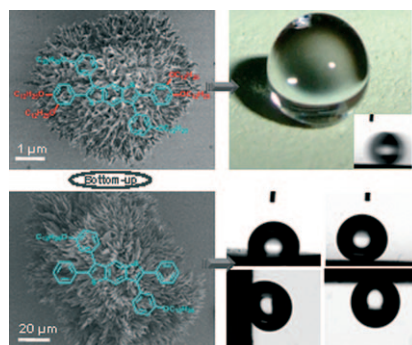


No drought here: Water-exchange reactions of $[\text{Zn}(\text{H}_2\text{O})_4\text{L}]^{2+} \cdot 2\text{H}_2\text{O}$ (L = imidazole, pyrazole, 1,2,4-triazole, pyridine, 4-cyanopyridine, 4-aminopyridine, 2-azaphosphole, 2-azafuran, 2-azathiophene, and 2-azaselenophene) have been studied by DFT calculations (B3LYP/6-311+G**) and provide theoretical evidence that the exchange mechanism follows a limiting associative reaction mechanism (see picture) to form a six-coordinate intermediate $[\text{Zn}(\text{H}_2\text{O})_5\text{L}]^{2+} \cdot \text{H}_2\text{O}$.

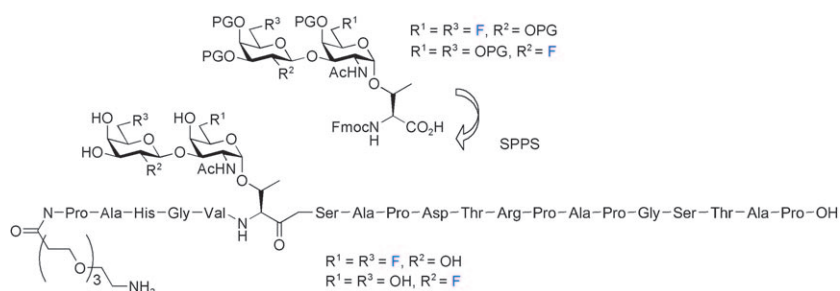
Superhydrophobicity

J. Yin, J. Yan, M. He, Y. Song,* X. Xu,
K. Wu,* J. Pei* 7309–7318

**Solution-Processable Flower-Shaped
Hierarchical Structures: Self-Assembly,
Formation, and State Transition of
Biomimetic Superhydrophobic
Surfaces**



Flower power! Two types of scales (micro and nano) of flower-shaped morphologies that exhibit excellent water-repelling characteristics have been formed from the hierarchical self-assembly of benzodithiophene derivatives (see figure). Because of the slight structural differences in the two kinds of flowers, a transition from the Cassie to Wenzel state was realized.



Fluorine in glycopeptides: Novel orthogonally protected fluorinated glycosyl amino acids have been prepared and incorporated into a glycopeptide sequence from the mucin MUC1 (see scheme). The resulting artificial

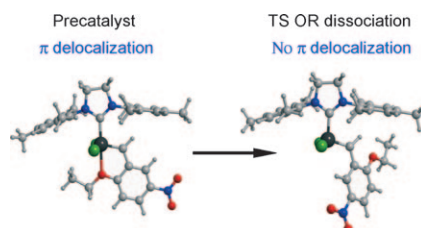
tumour-associated glycopeptides are suitable for further conjugation and might prove to be valuable vaccine building blocks with increased hydrolysis resistance.

Glycopeptides

S. Wagner, C. Mersch,
A. Hoffmann-Röder* 7319–7330

Fluorinated Glycosyl Amino Acids for Mucin-Like Glycopeptide Antigen Analogues

The ring cycle: DFT calculations on the full catalytic cycle of diene ring-closing metathesis by Ru-based Grubbs–Hoveyda-type complexes show that both the activity of the catalysts and their recovery depend on the π delocalization between the phenyl and the carbene in the precatalyst (see figure).



Density Functional Calculations

X. Solans-Monfort,* R. Pleixats,
M. Sodupe 7331–7343

DFT Mechanistic Study on Diene Metathesis Catalyzed by Ru-Based Grubbs–Hoveyda-Type Carbenes: The Key Role of π -Electron Density Delocalization in the Hoveyda Ligand

* Author to whom correspondence should be addressed

VIP Full Papers labeled with this symbol have been judged by two referees as being “very important papers”.

Supporting information on the WWW (see article for access details).

A video clip is available as Supporting Information on the WWW (see article for access details).

SERVICE

Spotlights 7058 Author Index 7344 Keyword Index 7345 Preview 7347

Issue 23/2010 was published online on June 14, 2010

CORRIGENDUM

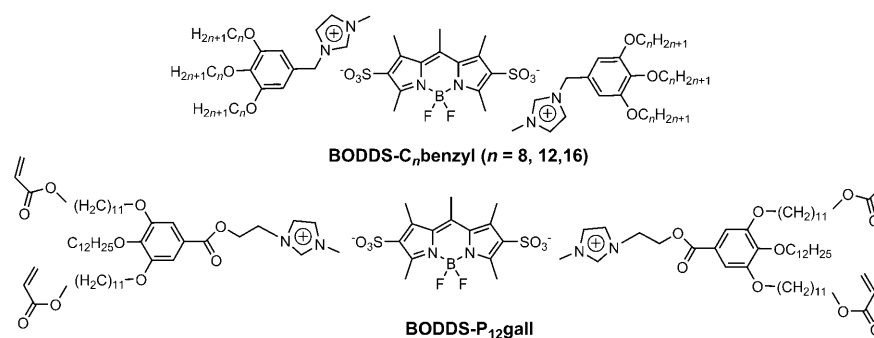
J.-H. Olivier, F. Camerel, G. Ulrich,
J. Barberá,* R. Ziessel* . . . 7134–7142

Luminescent Ionic Liquid Crystals from Self-Assembled BODIPY Disulfonate and Imidazolium Frameworks

Chem. Eur. J., 2010, 16

DOI: 10.1002/chem.201000339

The authors have noted that there is a mistake in Scheme 1 of this Full Paper. A corrected version of this scheme is included below. The authors apologize for this oversight.



Scheme 1. Structures of BODDS- C_n benzyl ($n=8, 12, 16$) and BODDS-P₁₂gall.